SURFACE AND INTERFACE ANALYSIS
Surf. Interface Anal. 2006; **38**: 1236–1241
Published online 19 June 2006 in Wiley InterScience
(www.interscience.wiley.com) DOI: 10.1002/sia.2385

Surface and Interface Analysis

Measuring the electronic structure of disordered overlayers by electron momentum spectroscopy: the Cu/Si interface

K. L. Nixon,[1] M. Vos,[2]* C. Bowles[2] and M. J. Ford[3]

[1] School of Chemistry, Physics and Earth Sciences, Flinders University, GPO Box 2100, Adelaide SA 5001, Australia
[2] Atomic and Molecular Physics Laboratory, Research School of Physical Sciences and Engineering, The Australian National University, Canberra ACT 0200, Australia
[3] Institute for Nanoscale Technology, University of Technology, Sydney, PO Box 123, Broadway, NSW 2007, Australia

Received 13 March 2006; Revised 24 April 2006; Accepted 25 April 2006

The Cu–Si interface was studied by electron momentum spectroscopy. A thick disordered interface is formed if one material is deposited on the other. Electron momentum spectroscopy measures intensity as a function of binding energy and target electron momentum. Momentum resolution is demonstrated to be very helpful in interpreting the data, even for these disordered interfaces. The interface layer has a well-defined electronic structure, different from either Si or Cu, and consistent with silicide formation. Information is obtained about the total bandwidth of the interface compound, effective Brillouin zone size and Fermi radius. No clear differences are observed in the electronic structure of the interface layer for Si deposited on Cu or Cu deposited on Si. Copyright © 2006 John Wiley & Sons, Ltd.

KEYWORDS: copper silicide; electron momentum spectroscopy

INTRODUCTION

The electronic structure of interfaces is an important subject in applied and fundamental physics. Often, one can grow the overlayers epitaxially and in that case the electronic structure can be studied by angular-resolved photoemission. Other interfaces are much more reactive, and a disordered layer is formed. For these cases, angular-integrated photoemission can be used to obtain the density of states, weighted by matrix elements. Although these measurements contain valuable information about the electronic structure, they do not provide information as rich as that obtained by angular-resolved photoemission for epitaxial layers.

There is an alternative, much less frequently used, technique that can measure momentum-resolved spectra: electron momentum spectroscopy (EMS).[1] This technique has been applied to measure the electronic structure of polycrystalline copper[2,3] and amorphous silicon samples,[4] and more recently single-crystalline silicon[5–7] and copper[8] samples as well. It relies on high-energy transfer collisions between an energetic incoming electron (energy of several 10's of keV) with a target electron, which is subsequently ejected from the sample. EMS uses thin films and both scattered and ejected electrons are detected in coincidence, and is hence also referred to as (*e*,2*e*) spectroscopy.

*Correspondence to: M. Vos, Atomic and Molecular Physics Laboratory, Research School of Physical Sciences and Engineering, The Australian National University, Canberra ACT 0200, Australia.
E-mail: maarten.vos@anu.edu.au

Of course, the anisotropy of the electronic structure can only be resolved using single crystals. For a polycrystalline sample EMS obtains angular-averaged spectra, which will generally be broader and show less structure than those obtained for a single crystal. However, these angular-averaged spectra often still contain detailed information, not contained in angular-integrated photoemission. For example, the Fermi surface of copper is almost spherical (radius k_f), except for deformations near the ⟨111⟩ directions. Hence for polycrystalline Cu samples, the intensity of an EMS measurement at the Fermi level is sharply peaked around momentum values k_f.

A case that is not affected by angular averaging is the spectrum measured at zero momentum. This spectrum should be identical for a single crystal and a polycrystalline sample. Here, the band structure usually has a maximum binding energy, and the zero momentum spectra will have a strong peak at this energy. The total bandwidth can thus be obtained more easily from EMS than from angular-integrated photoemission, as in the latter case it requires the determination of the extent of a low intensity tail relative to the secondary electron background.

In this paper, we want to study the formation of the copper/silicon interface. This technologically important case has been studied extensively by ultraviolet photoemission spectroscopy (UPS) and Auger spectroscopy. This interface is far from abrupt, and a thick disordered layer is formed. As we have studied pure silicon and copper extensively using EMS, we are in a good position to study the interface formed when Cu is deposited on a Si substrate or vice

WILEY InterScience® DISCOVER SOMETHING GREAT

Copyright © 2006 John Wiley & Sons, Ltd.

versa, and investigate to what extent the EMS measurements corroborate the interpretation of the results obtained with other techniques for the Cu/Si interface.

The literature of the Cu/Si interface is quite extensive, and we give here a very brief summary of the picture that emerges from this work. From UPS and Auger electron spectroscopy (AES) results, it was possible to characterize the changes in the valence signals from both copper and silicon upon the formation of a copper-silicon interface (e.g. Refs 9, 10). A change is seen in both the Si 3p and Cu 3d states upon the deposition of copper on a silicon substrate, and vice versa, which is most commonly attributed to a hybridization of these two states.[10] The change in width observed for the UPS Cu 3d peak is attributed to the variation in the number of nearest-neighbor-like atoms, resulting in a reduction in d–d hybridization.[11] The change in the lineshape of the Si 2p signal in X-ray photoemission spectroscopy (XPS) spectra is characteristic of the unresolved Si 2p doublet when silicon atoms are embedded in a metallic environment. Hence, their sp^3 configuration is disrupted and, therefore, they behave as metallic atoms. The split AES signal is due to changes in the local DOS around the silicon atoms, namely, the sp^3 hybrid Si–Si bonds are broken and replaced with Si-metal bonds.[12] This strongly suggests that copper and silicon have interdiffused and the Si atoms are now in a metallic environment. That behavior is similar to what was observed for Pd_2Si,[10] where the measured peaks were attributed to Si p-bonding states and partially occupied Si p-antibonding states were hybridized with the Cu 3d bonding and antibonding states. However, the identity of the silicide was brought into question when XPS results of the interface and Cu_3Si were shown to differ,[13] despite numerous studies showing the interface to have a 3 : 1 Cu : Si ratio.[10–12]

EXPERIMENTAL

The high-energy, high-resolution EMS spectrometer used, which is fully described elsewhere[14] is sketched in Fig. 1. The electron gun produces a 25 keV beam and the sample is in a high voltage sphere, kept at +25 keV. Thus, a (well-collimated) beam of 50 keV electrons is incident on a thin, self-supporting sample. Some of the incident electrons undergo a binary collision with a target electron and transfer a large fraction of their energy to this electron. If the incident and ejected electrons emerge with nearly equal energies (25 keV) and polar angles (∼45°) relative to the incident (z) direction, then they are detected in coincidence by two electrostatic analyzers, fitted with two-dimensional position-sensitive detectors.[14] The use of such high energies for the incident and emitted electrons greatly reduces the multiple scattering effects, which plagued earlier measurements.[15] Moreover, the incoming and outgoing electrons can be accurately treated as plane waves (i.e. have a well-defined momentum) in such a high-energy experiment. The energies and azimuthal angles of the emerging electrons are determined from their impact position at the two-dimensional position-sensitive detectors.[14] Knowing their energies E_i and angles (and hence momenta $\boldsymbol{k}_i$), one can infer the binding energy ω and momentum $\boldsymbol{q}$ of the struck electron before the collision through the conservation laws

$$\omega = E_0 - E_1 - E_2, \qquad \boldsymbol{q} = \boldsymbol{k}_1 + \boldsymbol{k}_2 - \boldsymbol{k}_0 \tag{1}$$

where the subscripts $i = 0$, 1, 2 refer to the incident and emitted (scattered and ejected) electrons, respectively.

If the mean scattering plane (horizontal plane) is defined as the $x - z$ plane, then the momentum component q_y is determined by the relative azimuthal angles ϕ_1, ϕ_2 of the two detected electrons. The momentum components in the x- and z-directions are determined by the choice of polar angles. In the present case, the polar angles were both fixed at $\theta_s = 44.3°$ for which choice $q_x = q_z = 0$. Different choices of polar angles near 44.3° give other values for q_x and q_z, in which case the measurements are along lines in momentum space that do not go through $q = 0$ (a Γ point).[14] Thus, after correction for detector efficiencies the outcome is in the form of a two-dimensional array q_y, ω, and we can plot either spectra: intensity as a function of binding energy for a given q_y value (and $q_x \cong q_z \cong 0$), or momentum densities for a given energy.

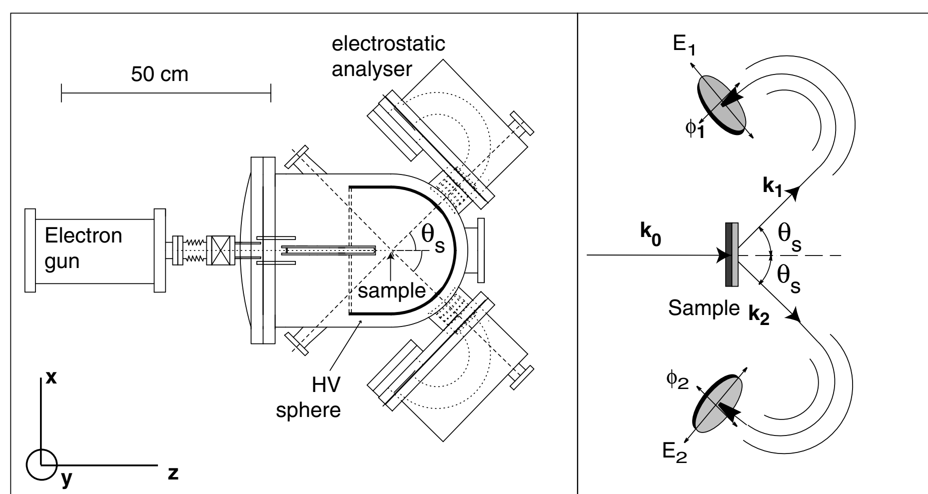

Figure 1. A schematic view of the EMS spectrometer of the Australian National University (left panel), and the incoming and outgoing beams relative to the sample. The reactive layer (lighter part of the sample) is at the analyzer side.

Copyright © 2006 John Wiley & Sons, Ltd.

Surface and Interface Analysis

In EMS, the measurement involves real momenta and it does not depend on the crystal lattice. This applies as well for (gas-phase) atoms and molecules, amorphous materials as it does for the present single-crystalline and polycrystalline samples. For the polycrystalline samples, we can measure the spherically averaged spectral function. The energy and momentum resolution are 1.0 eV and 0.1 a.u. respectively (1 a.u. of momentum corresponds to 1.89 $Å^{-1}$, 1 a.u. of length equals 0.529 Å). Energies quoted are relative to the Fermi level (valence band maximum for Si) as determined from the cut-off in the spectra. The accuracy of the Fermi level position determination is about 0.5 eV.

EMS is a transmission spectroscopy that requires extremely thin freestanding films. Hence, it is essential that the substrate is available as a thin film (around 100 Å). The thickness of the reacted layer, formed after deposition of the overlayer by evaporation, should be a considerable fraction of the thickness of the original thin film. Measurements are done with the reacted layer at the analyzer side. For (*e*, 2*e*) events in the substrate, the total electron path length in the sample is larger than that for those in the overlayer, and a larger part of the trajectories are at 25 keV, rather than 50 keV, with corresponding shorter elastic and inelastic mean free paths. Thus, there is a much larger probability of elastic and or inelastic scattering of the incoming and or outgoing electrons for (*e*, 2*e*) events in the substrate. Multiple scattering effectively moves most of the substrate signal from a well-defined position to a smooth background. Hence, the substrate signal is preferentially attenuated, and sharp features owing to the reacted layer will dominate the spectrum, even if the substrate layer and reacted layer are of comparable thickness.

Several experiments were done, using either silicon single crystal substrates on which copper was deposited, or copper single crystal substrates on which Si was deposited. The substrate preparation procedure was described elsewhere for both Si[16] and Cu[8] and the final thickness of the thin single crystal substrates was around 100 Å. However, owing to the statistical nature of sputtering, the thickness is not expected to be homogenous. At these thicknesses, we have a useful coincidence count rate (0.5–2 Hz). The (*e*, 2*e*) events without multiple scattering form well-defined features at certain binding energy-momentum combinations, whereas (*e*, 2*e*) events with multiple scattering contribute to a rather featureless background spread out over a large momentum-energy region. Thus, although multiple scattering has affected at least half of the coincidence counts, striking well-defined dispersing structures are observed in the experiment due to (*e*, 2*e*) events without multiple scattering.

The indicated thickness of the evaporated layer was obtained from a crystal thickness monitor, and refers to the thickness the deposited layer would have if no reaction took place.

RESULTS

Some examples of spectra obtained for silicon deposited on Cu are given in Fig. 2, together with the corresponding spectra measured for the Cu film before Si deposition, and an amorphous Si spectrum obtained in a separate experiment. At zero momentum, we see a peak at 9.1 ± 0.5 eV binding energy for Cu, 12.1 ± 0.5 eV for Si, and 11.3 ± 0.5 eV for the Si–Cu sample. These values are consistent with previous findings for the bottom of the band for Cu[8] and Si.[5] For the Si-on-Cu sample, the peak is at an intermediate position indicating that the occupied band width of the reacted layer is inbetween that of Cu and Si. For momenta in the 0.4–0.5 a.u. range, the Cu spectrum has again a peak at lower binding energy than the Si spectrum, but now there is a double peak in the spectrum of the Si-on-Cu sample. At even larger momenta (between 1.0 and 1.1. a.u.), the Si spectrum has a large intensity near the Fermi level, whereas the Cu and Si-on-Cu spectra have peaks at several eV from the Fermi level.

A simple interpretation is that the spectra of the Si-on-Cu sample is just the sum of that of a copper layer and a silicon layer. Indeed, we can get a reasonable fit of the spectra for $0 < |q| < 0.1$ a.u by taken a weighted

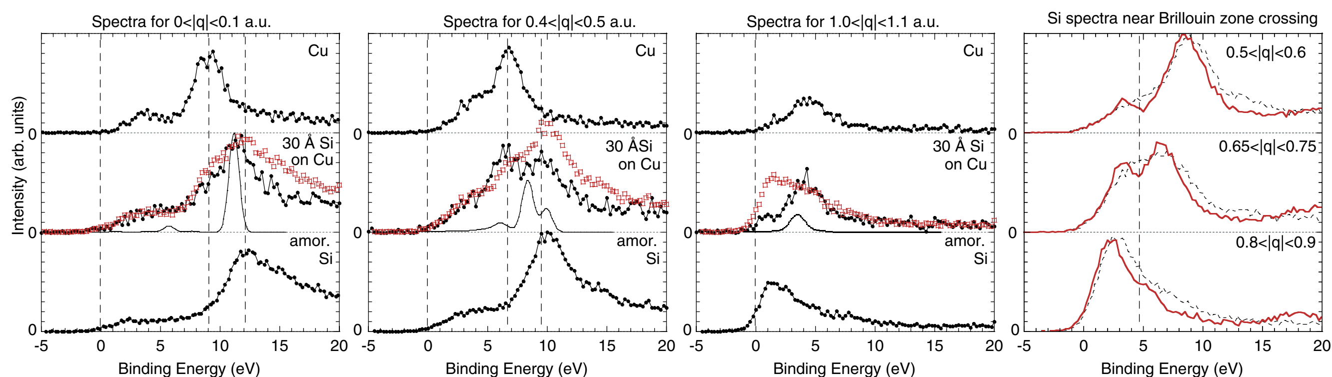

Figure 2. A comparison of the spectra of single crystal copper (top), amorphous silicon (bottom) and 30 Å silicon deposited on the Cu crystal (middle). The spectra near zero momentum (left panel) of the Si/Cu sample can be reasonably well described as the sum of a copper and amorphous Si (red, open symbols), but this sum fails completely to describe the spectra for $1.0 < |q| < 1.1$ a.u. (third panel). The spectra of the interface compound at $0.4 < |q| < 0.5$ a.u. (second panel) are characteristic of spectra taken near a Brillouin zone crossing. The solid line is the result of the CRYSTAL98 calculation convoluted with the estimate of the experimental resolution of 1 eV. For amorphous (black, dashed line) and crystalline Si (red thick line), we demonstrate the Brillouin zone crossing in the fourth panel.

Copyright © 2006 John Wiley & Sons, Ltd.

sum of the silicon spectrum and the copper spectrum at that momentum range. The open symbols in the first three panels of Fig. 2 are obtained from an 'empirical fit' using a weighted sum of 1/3 times the Cu spectrum plus 2/3 times the Si sample. An important advantage of EMS is that it does not just provide a single spectrum, but a set of spectra (one for each momentum) with the same normalization. Thus, if the sample consists of just a silicon layer and a copper layer, then the same weighted sum should describe the experimental data for all momentum values. The double maximum, seen in the Si-on-Cu sample at $0.4 < |q| < 0.5$ a.u. momentum range, would then be explained by the Si and Cu bands appearing at different energies. This fit is less satisfactory, but still somewhat reasonable. However, at larger momentum values $1.0 < |q| < 1.1$ a.u., the fit completely fails to describe the data, as the Si sample has in this momentum region considerable intensity near the valence band maximum, and the intensity of the Si-on-Cu sample is small at these energies.

Hence, we have to conclude that the measured intensity is not just from a Cu layer and a Si layer, but dominated by a reacted layer. Near zero momentum, the peak in the spectrum of the Si-on-Cu sample is then a measurement of the total band width. We will now suggest that the double-peaked structure seen in the $0.4 < |q| < 0.5$ a.u. momentum range is indicative of a Brillouin zone crossing, by comparing this structure with that seen for Si at larger momenta.

In the last panel of Fig. 2, we show the spectra near the Brillouin zone crossing for a crystalline silicon substrate (rotated away from high symmetry directions), and for an amorphous Si sample measured in a separate experiment. In the 0.65–0.75 a.u. momentum range, we see a clear double peak structure for the crystalline Si sample; for the amorphous sample the double structure is washed out, but its remnants still cause a flat-peaked structure in the 0.65–0.75 a.u. momentum spectrum. For amorphous Ge, the double-peaked structure persists in the amorphous phase.[17] For Si and Ge, we know that these double-peaked structures in the 0.65–0.75 a.u. momentum range are because of Brillouin boundary crossings, and hence, we interpret the similar double-peaked structure for the Si-on-Cu sample as again an indication of a Brillouin Zone crossing. As the unit cell of Si is smaller, the volume of its Brillouin zone is larger, and the Brillouin zone crossing appears in the Si sample at larger momenta than in the Si-on-Cu sample. Thus, this suggests that the average distance from zero momentum to the first Brillouin zone boundary for the compound formed in the Si-on-Cu sample is around 0.45 a.u. (0.84 $Å^{-1}$). Similar double-peaked structures were found at the same momentum range for experiments in which Cu was deposited on a Si substrate.

In Fig. 2, we also show the calculated spectra for Cu_7Si_2 as obtained from the CRYSTAL98 suite of programs,[18] where crystalline orbitals are generated self-consistently from density-functional theory (DFT) applied to linear combinations of atomic orbitals (LCAO). The local density approximation (LDA) with Vosko-Wilk-Nusair exchange and correlation[19] were employed for the exchange-correlation functional. It is expected that the LDA will give sufficient agreement as far as the dispersion of the peak positions is concerned for the present, qualitative comparison. High-quality, all-electron basis sets recommended by the authors of CRYSTAL98 were used; that is 86-4111(41d)G and 66-21G* for copper and silicon respectively. A relatively dense k-point grid was employed and total energies are well converged. Default tolerances for the CRYSTAL98 code were used for other computational parameters, again giving well-converged total energies and band structures.

The crystal structure of copper precipitates in silicon were determined by Solberg.[20] The room temperature η'' phase (Cu_3Si) has a 2-dimensional long period superlattice crystal with stacking faults and vacancies. This makes it very hard to model computationally because of the very large number of atoms in the unit cell and the disordered structure. This η'' phase is thought to be based on the intermediate temperature η' phase of Cu_7Si_2.[20] This structure is compact and ordered and therefore more computationally amenable. The η'' and η' phases have similar local environments. Since the electronic structure is largely dependant on the local environment, the simpler η' phase (Cu_7Si_2) was thought to be a good approximation of the η'' phase. Hence, following Magaud *et al*.[21] we use this phase for our calculations.

It is seen in Fig. 2 that the total bandwidth is well described by the theory (i.e. the theory describes the peak position in the spectra at zero momentum well). However the band gap behavior, as shown in the spectra for $0.4 < q < 0.5$ a.u., is qualitatively different. Even after spherically averaging (to account for the expected polycrystalline structure of the copper-silicon), the calculations show three maxima in intensity separated by minima at 7 eV and one at 9 eV. In the experiment, we see two maxima separated by a single, broader minimum in intensity, centered around 8 eV. This could be a sign that the long-range order of the Cu_7Si_2 or similar phase is not fully established in the reacted layer.

In Fig. 3, we plot the momentum densities, but now for the reverse case: a 50-Å thick Cu layer deposited on a thin crystalline Si film. We also plot the momentum densities of the Si film before Cu deposition, and the polycrystalline Cu momentum density, obtained in a separate experiment. Near E_f, all three spectra are peaked at distinct momentum values, Cu at the smallest ($|q| = 0.70 \pm 0.05$ a.u.), Si at the largest ($|q| = 1.0 \pm 0.05$ a.u.), and the Cu–Si sample at intermediate values ($|q| = 0.80 \pm 0.05$ a.u.). The momentum density of the Cu–Si sample is too sharp to be the sum of the Cu momentum density and the Si momentum density. Thus, again a surface layer is formed with a distinct electronic structure. The density of the Cu–Si sample has shoulders at the large momentum side of the peaks, aligning with the Si momentum density at E_f, which is probably because of the Si substrate.

In a first-order approximation, treating the valence sp electrons as free electrons, one can calculate the Fermi vector from the number of sp electrons N_{sp} per unit cell volume V:

$$k_f = \left(\frac{3\pi^2 N_{sp}}{V}\right)^{1/3} \quad (2)$$

Assuming 1 s electron per unit cell we obtain $k_f = 0.71$ a.u. for Cu. For the Cu_7Si_2 compound (1 s electron per Cu

Copyright © 2006 John Wiley & Sons, Ltd.

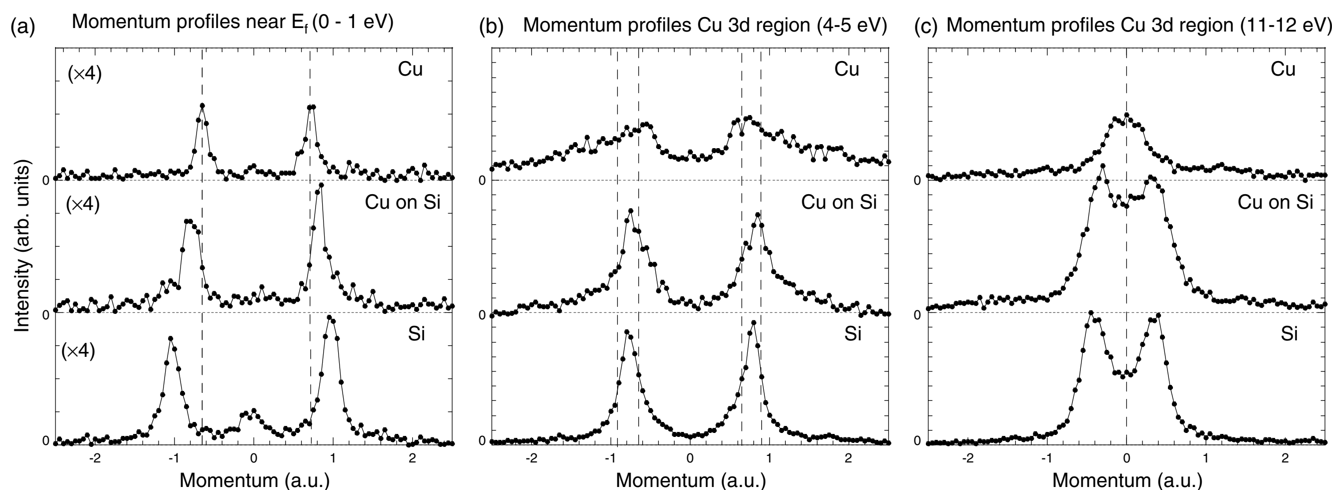

Figure 3. Momentum profiles near the Fermi level for polycrystalline copper (a), 50 Å copper on silicon (b) and crystalline silicon (c). The separation of the peaks at the Fermi level is also quite distinct for each of the samples, indicating different sp electron densities within each sample. The central panel shows the momentum profiles in the 4–5 eV binding energy region, and the right panel shows the profiles for 11–12 eV binding energy, below the bottom of the Cu band, but above that of Si and the Cu–Si samples.

atom, 4 sp electrons per Si atom) and its unit cell of 310 $Å^3$, (containing 6 Si atoms and 21 Cu atoms), we obtain $k_f = 0.85$ a.u. For Si, a semiconductor, for which this model is less applicable, one obtains $k_f = 0.96$ a.u. This is in reasonable agreement with the experiment, and the observations at the Fermi level can be explained qualitatively in a simple, intuitive, way.

In the 4–5 eV binding energy, the momentum density of Cu looks completely different. In the 3d region where the bands are rather flat, i.e. there is only a small change in binding energy with changing momentum; as a consequence there are no sharp peaks in the momentum density of polycrystalline Cu at these binding energies. For the Si case, dispersion is still strong, and sharp peaks are obtained, with very little intensity at large momentum values. This is characteristic of a sp-bonded solid. The momentum density of the Cu–Si sample is inbetween these two cases. There are clear peaks, but broader than those of Si, and there is considerable intensity extending to large magnitudes of momentum, indicating the presence of d electrons.

Finally, for 11–12 eV binding energy, the shape of the momentum profiles have changed again. Now we are close to the bottom of the valence band. For most solids, this part of the band structure occurs at zero momentum. Dispersion generally has a parabolic shape here, reflecting the decrease in binding energy with increasing kinetic energy. For Cu, we are now below the bottom of the band and hence we would naively expect no intensity, and the fact that we still observed a nonzero intensity is due to lifetime broadening of the electronic states and finite energy resolution of the spectrometer. For the Si sample, we are still above the bottom of the band and the momentum densities still have a well-separated maximum away from zero momentum. For the alloy system, we are approaching the bottom of the band and the positive and negative momentum components are starting to merge.

DISCUSSION AND CONCLUSIONS

We have demonstrated that EMS can provide a large amount of information about electronic structures of disordered layers that form during reactive interface formation. As this is a transmission technique, it requires that thin free-standing samples are available and that the thickness of the reacted layer is comparable to that of the remaining substrate layers. These are fairly severe restrictions, but for the Cu–Si interface all these conditions are met.

The fact that EMS does not just provide intensity as a function of energy ω but measures intensity as a function of (ω, q_y) limits the possible interpretations. This was illustrated by the fact that the spectrum at $0 < |q_y| < 0.1$ a.u. could be described by the sum of a Cu contribution and a Si contribution, but the intensity near $1.0 < |q_y| < 1.1$ a.u. could not be described by the same sum. Thus, we can conclude that the signal mainly originates from a reacted layer. Spectra obtained for Cu deposited on Si were similar to those obtained for Si on Cu, in agreement with previous literature,[22] indicating that reacted layers formed in both experiments have similar compositions. A thicker Cu layer has to be deposited on Si before the characteristic spectra of the reacted layer was observed, consistent with a Cu rich stoichiometry of the reacted layer. In spite of the polycrystalline nature of this layer, we could determine the total bandwidth from the spectrum at $q_y = 0$; we could infer the approximate average size of the Brillouin zone from the characteristic double peak structure around $0.4 < |q| < 0.5$ a.u. and determine the average Fermi level radius. Generally, the results appear consistent with silicide formation at the interface.

The spectrometer used here, with very similar energies for the ejected and scattered electrons, is suitable for the study of interfaces with a thick reacted layer. Spectrometers employing a more asymmetric kinematics (energy of the ejected electron much smaller than that of the scattered electron), such as the spectrometer described by Storer *et al.*,[23] are in principle suitable for the study of thinner reacted layers. Owing to the lower incoming energy of

Copyright © 2006 John Wiley & Sons, Ltd.

this spectrometer ($E_0 \cong 20$ keV), its use is limited to the thinnest of free-standing films. A 100 keV spectrometer, with scattered and ejected electrons at energies near 99 keV and 1 keV, would make the study of a much larger range of interfaces possible, as information is obtained from a thickness determined by the mean free path of 1 keV electron, but the allowed total thickness of the sample is of the order of the mean free path of a 100 keV electron.

Acknowledgements

This research was made possible by support of the Australian Research Council. K.L.N. acknowledges support by the Ferry Scholarship Trust. The authors thank Michael Went for critically reading the manuscript.

REFERENCES

1. Weigold E, McCarthy IE. *Electron Momentum Spectroscopy*. Kluwer Academic/Plenum: New York, 1999.
2. Guo X, Fang Z, Kheifets AS, Canney SA, Vos M, McCarthy IE, Weigold E. *Phys. Rev., B* 1998; **57**: 6333.
3. Kheifets AS, Vos M, Weigold E. *Z. Phys. Chem. (Muenchen)* 2001; **215**: 1323.
4. Vos M, Storer P, Cai Y, Kheifets A, McCarthy I, Weigold E. *J. Phys.: Condens. Matter* 1995; **7**: 279.
5. Sashin VA, Canney SA, Ford MJ, Bolorizadeh MA, Oliver DR, Kheifets AS. *J. Phys.: Condens. Matter* 2000; **12**: 125.
6. Vos M, Bowles C, Kheifets AS, Sashin VA, Weigold E, Aryasetiawan F. *J. Electron Spectrosc. Relat. Phenom.* 2004; **137–40**: 629.
7. Vos M, Bowles C, Kheifets AS, Went MR. *Phys. Rev. B* 2006; **73**: 085207.
8. Vos M, Kheifets A, Bowles C, Chen C, Weigold E, Aryasetiawan F. *Phys. Rev. B* 2004; **70**: 205111.
9. Abbati I, Grioni M. *J. Vac. Sci. Technol.* 1981; **19**: 631.
10. Rossi G, Kendelewicz T, Lindau I, Spicer WE. *J. Vac. Sci. Technol. A* 1983; **1**: 987.
11. Cros A, Aboelfotoh MO, Tu KN. *J. Appl. Phys.* 1990; **67**: 3328.
12. Ringeisen F, Derrien J, Daugy E, Layet JM, Mathiez P, Salvan F. *J. Vac. Sci. Technol. B* 1983; **1**: 546.
13. Corn SH, Falconer JL, Czanderna AW. *J. Vac. Sci. Technol. A* 1988; **6**: 1012.
14. Vos M, Cornish GP, Weigold E. *Rev. Sci. Instrum.* 2000; **71**: 3831.
15. Vos M, Bottema M. *Phys. Rev. B* 1996; **54**: 5946.
16. Utteridge SJ, Sashin VA, Canney SA, Ford MJ, Fang Z, Oliver DR, Vos M, Weigold E. *Appl. Surf. Sci.* 2000; **162–163**: 359.
17. Bowles C, Went M, Kheifets A, Vos M. *AIP Conf. Proc.* 2006; **811**: 167.
18. Saunders V, Dovesi R, Roetti C, Caus M, Harrison N, Orlando R, Zicovich-Wilson CM. *CRYSTAL98 User's Manual*. Università di Torino: Torino, 1999.
19. Vosko SH, Wilk L, Nusair M. *Can. J. Phys.* 1980; **58**: 1200.
20. Solberg JK. *Acta Crystallogr., Sect. A* 1978; **34**: 684.
21. Magaud L, Guillet S, Lopez-Rios T. *Physica B* 1996; **225**: 225.
22. Rojas C, Román E, Martín-Gago JA. *Surf. Interface Anal.* 2000; **30**: 570.
23. Storer P, Caprari RS, Clark SAC, Vos M, Weigold E. *Rev. Sci. Instrum.* 1994; **65**: 2214.

Copyright © 2006 John Wiley & Sons, Ltd.